

24. PALEOMAGNETISM OF CRETACEOUS BASALTS FROM THE EAST MARIANA BASIN, WESTERN PACIFIC OCEAN¹

Brian P. Wallick² and Maureen B. Steiner³

ABSTRACT

Cretaceous basalts have been recovered at several Ocean Drilling Program and Deep Sea Drilling Project sites where basement of Jurassic age was predicted. Sites 800 and 802, Leg 129, both fall in this category. We have examined the paleomagnetic properties of 25 basalt samples from Site 802 in order to establish a paleolatitude for the site at the time of basalt emplacement and to compare the results to those from Deep Sea Drilling Project Site 462. Mean natural remanent magnetization intensity for the Site 802 basalts was found to be approximately 12 A/m consistent with typical oceanic basalts. Mean stable inclination is $-34.7^\circ \pm 2.2$ which implies a paleolatitude of approximately 19.4° S. This is very similar to the paleolatitudes calculated for Site 462 basalts and suggests—along with similarities in geochemistry, magnetic properties, and projected age of Site 802 basalt emplacement—both contemporaneity of and a possible source link between the two sites.

INTRODUCTION

The search for Jurassic basement within the confines of the Jurassic Magnetic Quiet Zone has been fraught with a variety of problems, not least of which is the recovery of basalts and dolerites of an age inconsistent with that predicted from observed magnetic anomaly patterns. For example, Deep Sea Drilling Project (DSDP) Hole 462A ($7^\circ 14.5'N$, $165^\circ 1.9'E$) was drilled in the Nauru Basin just north of what was interpreted to be magnetic anomaly M26, which suggests a Late Jurassic age for the site (Larson et al., 1981). The first leg to drill the site, Leg 61, discontinued drilling after recovery of some 500+ m of Cretaceous volcanics (Larson et al., 1981); reentry of Hole 462A on Leg 89 penetrated an additional 137 m of early Aptian or older basalt without encountering sediments or basement rocks of the predicted Jurassic age (Moberly et al., 1986).

The drilling results of Leg 129 yielded similar results for two of three sites, Site 800 ($21^\circ 55.4'N$, $152^\circ 19.4'E$) in the Pigafetta Basin and Site 802 ($12^\circ 5.8'N$, $153^\circ 12.6'E$) in the East Mariana Basin. Of particular interest is Site 802, which was drilled in the "Jurassic Quiet Zone"—a region presumed to be older than polarity chron M33 (Handschumacher et al., 1988) and hence having a predicted age of Middle Jurassic (Lancelot et al., 1990). Drilling at this site was terminated after penetration of 44 m of late Aptian extrusive basalts.

Examination of the paleomagnetic parameters of the extrusive basalts from Site 802 provides an opportunity to place a paleolatitude on the site at the time of emplacement. In addition, comparison of the properties of these materials with those recovered at Site 462 in the Nauru Basin provides possible insight into the relationship between these two sites.

METHODS

A total of 25 samples were taken from fine-grained basalt cores of Hole 802A. Of 17 flow units identified on board (Shipboard Scientific Party, 1990), 13 were sampled, the remainder being either too coarse-grained or too poorly represented (Fig. 1). While the sampling statistics do not adequately negate the effects of secular variation, a sufficient

number of flow units were sampled to allow characterization of the paleomagnetic properties of this portion of the volcanic pile. Samples consisted of 2.5-cm-diameter minicores drilled perpendicular to the drill core axis. Sampled intervals and their associated igneous unit designations are listed in Table 1.

All measurements of stepwise demagnetization were performed using a Schonstedt SSM-1 spinner magnetometer; six spin orientations were performed on each sample in order to minimize measurement error. Demagnetization was accomplished using a Schonstedt GSD-1 single-axis alternating field (AF) demagnetizer with incremental steps carried from 2.5 mT to a maximum of 65 mT. The majority of samples were reduced to less than 10% of their initial magnetization. Susceptibility was measured using a Bison MS-3 magnetic susceptibility bridge. All magnetic measurements are given in SI units with appropriate conversions as discussed by Shive (1986).

RESULTS

Intensity of Magnetization

Measurements of natural remanent magnetization (NRM) intensity (J_0) yielded a range of values between 0.6 and 28.8 A/m with an average of approximately 12 A/m. The range of values is quite similar to that observed in other oceanic basalts such as those recovered from Hole 504B (Furuta and Levi, 1983). The variation of NRM intensity with depth is shown graphically in Figure 2 and, in general, shows no systematic trend with depth over the length of the hole. Conversely, variation of NRM intensity from the mean appears to be largely a function of flow morphology and, to some extent, composition.

Three different patterns of intensity decay were noted in the stepwise demagnetization results. The first pattern is represented by a change in intensity of <10% on the first and/or second AF demagnetization step (2.5, 5.0 mT) followed on subsequent steps by more substantial intensity drops (Fig. 3A). This type of decay was noted in 13 of the 25 samples. Median destructive field (MDF) values for these samples range from 7.3 to 12.7 mT and average approximately 9.8 mT. A second type of decay was marked by the removal of approximately 20% of the sample magnetic intensity upon the 2.5-mT AF demagnetization step (Fig. 3B). Found in five samples, lower coercivity of remanence and hence lower stability is indicated. MDF values for these samples are much lower, as expected from their rapid decay, and range from 4.6 to 5.8 mT. The third type of decay (Fig. 3C) was marked by an increase in intensity at the first demagnetization step and suggests the removal of a weak, laboratory or drilling remanence vector. After these increases in intensity were recognized,

¹Larson, R. L., Lancelot, Y., et al., 1992. *Proc. ODP, Sci. Results*, 129: College Station, TX (Ocean Drilling Program).

²Department of Earth and Atmospheric Science, Purdue University, West Lafayette, IN 47907, U.S.A.

³Department of Geology and Geophysics, University of Wyoming, Laramie, WY 82701, U.S.A.

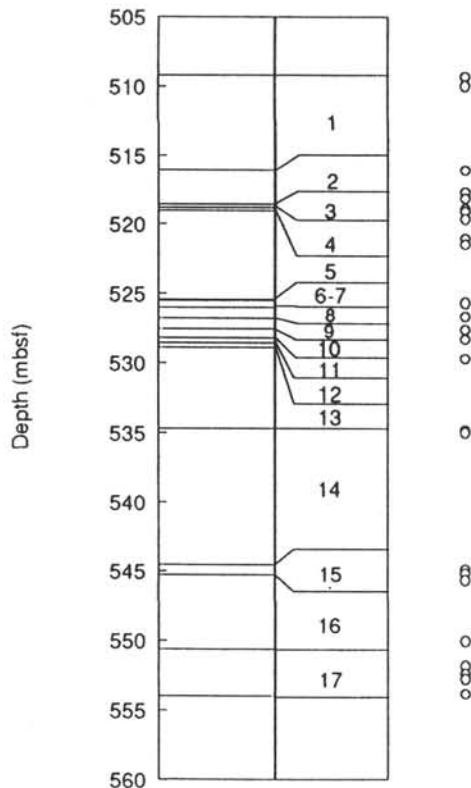


Figure 1. Basalt flow unit designation as defined by shipboard igneous petrology (Shipboard Scientific Party, 1990). The left and right columns represent the thickness and number designation of individual flow units, respectively. The open circles represent sampled intervals.

the NRM measurements of remaining, as yet undemagnetized, samples were repeated (see Appendix); these measurements showed an initial increase in intensity between the two NRM measurements similar to that seen in the single, low-field step of AF demagnetization. With no recognized consistency in direction of the vector removed, and the removal of the vector occurring with only one additional day of zero-field cleaning (i.e., short relaxation time), the weak remanence seems likely the product of storage rather than an *in-situ* viscous remanence.

MDF values for this previously described group ranged widely. However, when the 2.5-mT AF step intensity was substituted for J_0 , MDF values were significantly reduced in both magnitude and variance, from 8.2 to 14.1 mT with an average value of 9.7 mT. The resulting close correspondence of the range and mean of the MDF values of these samples to those of the first-described decay pattern suggests that the AF 2.5-mT demagnetization step may be a suitable approximation for the *in-situ* NRM values in this group. While the values of initial NRM measurements can be seen in the compiled results of Table 1 and in the stepwise measurements listed in the Appendix, all subsequent calculations of both MDF and Koenigsberger ratio for samples exhibiting such an intensity increase (marked with a star in Table 1) will use the 2.5-mT AF step as a substitute for the initial laboratory NRM.

Susceptibility

The susceptibility (χ) values of Site 802 basalts is between 1.75×10^{-2} and 3.33×10^{-2} SI, with a mean value of $2.48 \times 10^{-2} \pm 0.4 \times 10^{-2}$. Higher values of susceptibility for the flow (mean value, $2.99 \times 10^{-2} \pm 0.3 \times 10^{-2}$) are probably associated with an increase in grain size. In general, there is a direct relationship between grain size and susceptibility (e.g., Nagata, 1961; Stacey and Banerjee, 1974) corre-

sponding to the change in properties between single and multiple magnetic domains. The two flow morphologies can therefore be separated on the basis of susceptibility.

Stable Inclinations

The results of progressive AF demagnetization, vector decay curves, and declination-inclination stability were analyzed by using a combination of stereographic projection and vector-projection plots. Least squares analysis was applied to the vectors comprising stable declination-inclination values using the method developed by Kirschvink (1980). The results are given in Table 1.

Vector decay paths established during AF demagnetization (above 2.5 mT) were quite uniform (Fig. 4). The resultant inclinations were weighted using a method similar to that described by Ogg et al. (1991) and the mean inclination was computed for the sample suite. Since Ocean Drilling Program (ODP) drilling samples are azimuthally unoriented, the mean inclinations were calculated using the method of Kono (1980), a method which assumes that the statistics of inclination data mirrors a Fisherian distribution to magnetic directions. The basalt flows yielded a mean inclination of $-35.1^\circ \pm 2.5^\circ$, implying a paleolatitude of $19.4^\circ S \pm 1.7^\circ$. The polarity of the samples was interpreted as normal and, because of negative inclination values, assumes a Southern Hemisphere origin; this inference is consistent with the southern latitude setting determined for the overlying sediments (Shipboard Scientific Party, 1990; Steiner and Wallick, this volume).

While the value given for the mean inclination provides an estimate of the paleolatitude at the time of extrusion, the basalt pile may not reflect an average of a complete secular variation cycle. The estimated value for the precision parameter $K = 95.5$ from the above statistics gives an angular standard deviation of $S = 8.3^\circ$. The predicted value for S for the 80- to 110-Ma interval (Irving and Pullaiah, 1976) was found to be 12.6° for the calculated 19.4° latitude, and therefore suggests that, while very similar, sampling of flows at Site 802 may be insufficient to have completely removed the effects due to secular variation. Still, the difference of less than 5° between these two values of the angular standard deviation indicate the calculated paleolatitude may be considered a reasonably close approximation.

DISCUSSION

It is not possible to establish whether any structural rotation has occurred in the volcanic pile sampled at Site 802; indications from bedding in the overlying sedimentary rocks and from the drilling record show no evidence of severe wander in the drill hole before entry into the basalt column. Therefore, as a first approximation, the $19.4^\circ S$ value for the paleolatitude of Site 802 at the time of the extrusion of the basalts appears reasonable even though the section does not completely cover a paleosecular variation interval. Projecting the basalt paleolatitude, along with the paleolatitudes computed for the overlying sediments, gives an age in excess of 120 Ma (Kent and Gradstein, 1985) for the emplacement of these basalts, appreciably higher than the 114.6-Ma date determined by Pringle (this volume); this latter age is consistent with an age predicted by paleontology (Ogg, this volume). This discrepancy between the basalt paleolatitude and subsequent age projection and the sediment paleolatitude, paleontologic, and radiometric age data may be partly eliminated by assuming that a complete sampling of the volcanic pile, including a complete secular variation cycle, may give a lower overall value for the paleolatitude and hence a younger predicted age.

A reevaluation of paleontologic evidence for the age of Hole 462A interbasalt, radiolarian-bearing sediments (Shipboard Scientific Party, 1986; Schaaf, 1986) suggests deposition during the early Aptian, or approximately 118 Ma; this early Aptian age agrees with the early end of a 110- to 120-Ma spectrum given to the Nauru basalts by Ozima et al. (1981), while conflicting with more recent work by Pringle (this volume), who determined a 110-Ma basalt age. These data suggest age differences between Site 802 and Site 462 range from 6 m.y. based on paleontology,

Table 1. Results of paleomagnetic analysis.

Sample (cm)	Flow unit	Depth (mbsf)	J_{NRM} (A/m)	I_{NRM} (degrees)	MDF (mT)	J_s (A/m)	I_s (degrees)	χ ($\times 10^{-2}$)	Q
129-802A-									
⁴ 57R-2, 119	1	500.29	16.5	-1.8	9.9	3.0	-20.6	2.49	19.8
57R-3, 32	1	509.92	28.5	-28.9	9.9	11.5	-30.0	2.27	37.6
58R-1, 6	2	516.06	19.8	-35.0	7.3	8.5	-35.5	2.42	24.5
58R-2, 15	2	517.65	3.9	-27.9	5.7	0.6	-35.6	2.86	4.1
58R-2, 61	2	518.11	6.5	-37.6	4.6	0.5	-39.0	2.65	7.3
58R-2, 13	4	518.84	15.6	-32.6	12.7	8.5	-31.1	2.47	18.9
58R-3, 6	5	519.00	8.1	-38.2	12.5	4.3	-38.5	2.29	10.6
58R-3, 58	5	519.58	11.8	-35.8	4.9	2.4	-36.0	2.77	12.8
⁴ 58R-4, 51	5	521.01	8.9	-17.2	8.6	2.8	-19.3	2.53	10.5
⁴ 58R-4, 92	5	521.42	0.6	-21.9	8.3	2.9	-21.0	2.47	0.7
⁴ 59R-1, 20	7	525.60	3.4	25.8	9.8	1.4	-32.7	1.86	5.5
⁴ 59R-1, 119	8	526.59	3.8	-46.1	9.1	1.5	40.8	1.75	6.5
⁴ 59R-2, 63	10	527.53	16.1	28.8	14.1	14.1	-41.5	2.15	22.4
⁴ 59R-2, 135	11	528.25	4.7	-5.1	9.7	3.1	-28.8	2.57	5.5
59R-3, 124	13	529.64	12.2	-46.9	9.9	4.1	47.4	2.28	16.0
60R-1, 7	14	534.77	9.6	43.7	9.3	2.4	-45.0	2.26	12.7
60R-1, 26	14	534.96	14.8	-42.3	12.3	0.4	-31.3	2.08	21.2
61R-1, 70	15	544.90	28.8	-34.4	8.7	7.3	-34.3	2.24	38.5
61R-1, 95	15	545.15	26.8	-32.3	8.9	7.9	-32.9	1.88	42.6
61R-1, 145	16	545.65	17.7	-30.9	8.5	4.4	-31.5	2.65	20.0
62R-1, 92	17	550.02	8.4	-33.5	5.3	1.8	-34.6	2.73	9.2
⁴ 62R-1, 121	17	551.81	4.6	-20.0	8.2	1.4	-30.0	3.24	4.3
62R-2, 27	17	552.37	5.4	-22.5	5.8	0.5	41.5	3.33	4.8
62R-2, 64	17	552.74	10.3	-28.4	9.7	1.5	-38.3	2.96	10.4
62R-3, 23	17	553.83	11.3	-34.3	4.7	0.8	44.4	2.70	12.5

Notes: J_{NRM} = natural remanent magnetization intensity, I_{NRM} = NRM inclination, J_s = average stable intensity, I_s = stable inclination, χ = susceptibility, Q = Koenigsberger ratio.
^aSamples in which the second AF step showed a rise in intensity; calculations of MDF and Q for these samples are based on the second or 2.5-mT AF step as described in the text.

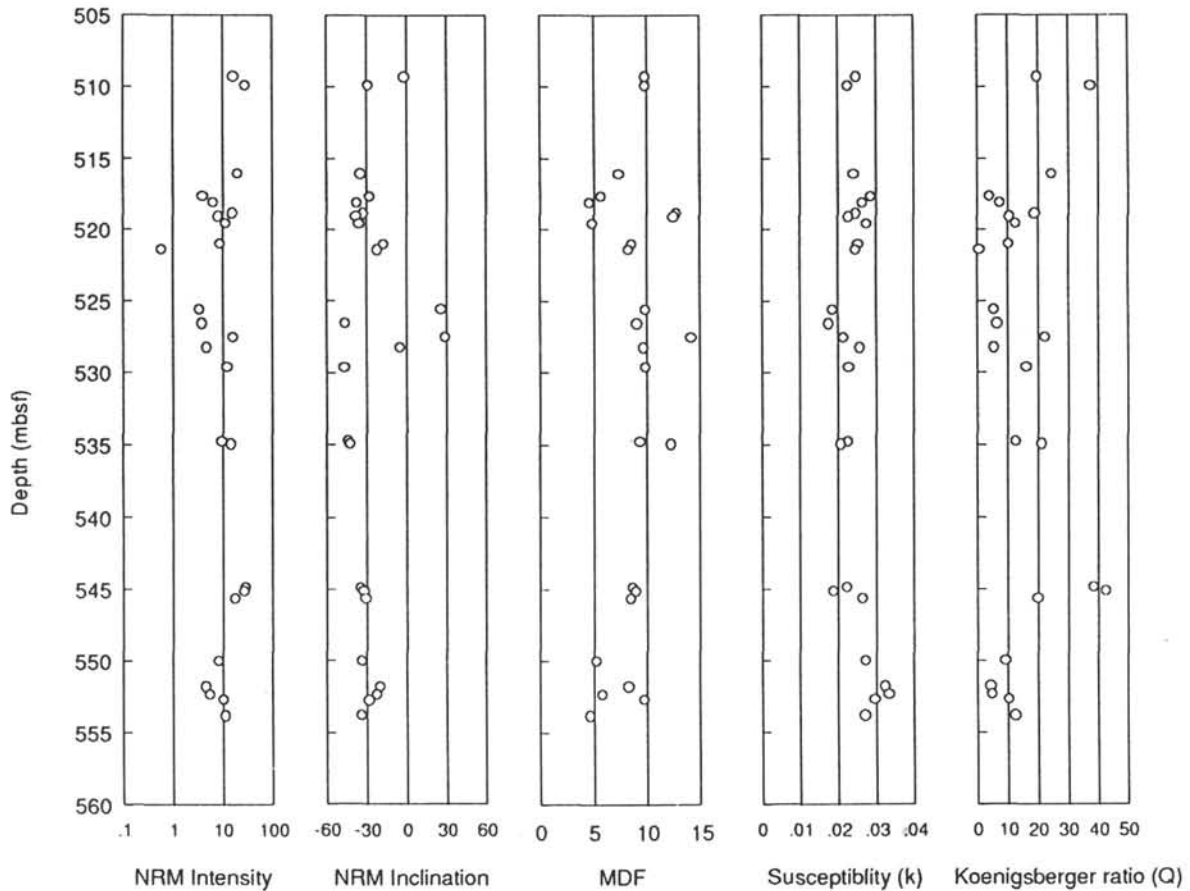


Figure 2. Changes in the magnetic parameters of NRM intensity, inclination, median destructive field (MDF), volume susceptibility, and Koenigsberger ratio with depth.

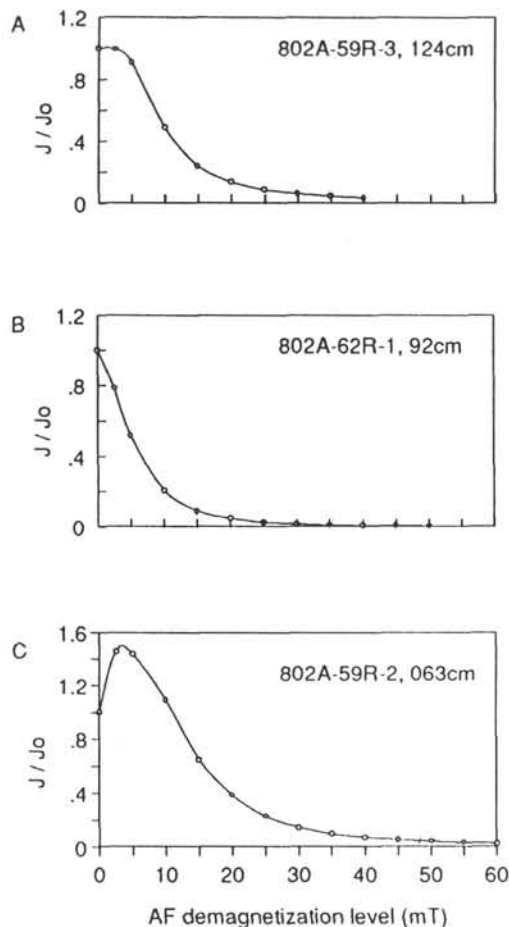


Figure 3. A–C. Demagnetization plots showing typical decay patterns of three distinct groups of samples. Values for J and J_0 are provided in the Appendix under the appropriate sample number. Details are provided in the text.

approximately 4 Ma based on radiometric ages, and contemporaneity based on paleolatitude projections.

The magnetic properties of the basalt flows at the two sites show similarities with comparable average median destructive fields, susceptibilities, and NRM intensities (Shipboard Scientific Party, 1986; Steiner, 1981). Additionally, there are pronounced geochemical similarities between the two sites (Castillo, this volume). Current latitudinal separation between the two sites is approximately 5° ; paleolatitudes of between 19.9° and 20.6° calculated for Hole 462A (Shipboard Scientific Party, 1986) are only slightly southward of those of the present work (19.4°). It is difficult, however, to relate the results of Hole 462A to this present work. From the work of Steiner (1981) and Ogg (in Shipboard Scientific Party, 1986), it is apparent that basalt flow inclinations fall into two groups: shallow ($<25^\circ$) and steep ($>35^\circ$). This may be due to lithology, paleosecular variation in recording of differently timed events (extrusive vs. intrusive), or, perhaps, overall crustal structure. If the estimates for the paleolatitude for Hole 462A are reasonable, then it may be concluded that the two sites were formed with today's approximate separation and the missing 5° of latitudinal difference is simply due to statistical sampling. If the sites are roughly contemporaneous, this would further suggest that the sites have moved along similar paths since their emplacement and may have shared a common source.

CONCLUSIONS

We offer the following conclusions regarding the Cretaceous basalts:

1. NRM intensities for these basalts averaged approximately 12 A/m, comparable to that of other oceanic basalts.
2. The average values for the median destructive field (9.8 mT) and initial susceptibility (2.4×10^{-2}) suggest that, for the most part, the basalt remanence is highly stable and indicate that measured NRM intensities are probably representative of *in-situ* values.
3. The paleolatitude calculated from mean paleomagnetic inclinations gives a value of $19.4^\circ \pm 1.7^\circ$, only slightly northward of the 19.9° and 20.6° reported for Hole 462A.

REFERENCES

- Furuta, T., and Levi, S., 1983. Basement paleomagnetism of Hole 504B. In Cann, J. R., Langseth, M. G., Honnorez, J., Von Herzen, R. P., White, S. M., et al., *Init. Repts. DSDP*, 69: Washington (U.S. Govt. Printing Office), 697–703.
- Handschumacher, D. W., Sager, W. W., Hilde, T.W.C., and Bracey, D. R., 1988. Pre-Cretaceous tectonic evolution of the Pacific plate and extension of the geomagnetic polarity reversal time scale with implications for the origin of the Jurassic "Quiet Zone." *Tectonophysics*, 155:365–380.
- Irving, E., and Pullaiah, G., 1976. Reversals of the geomagnetic field, magnetostratigraphy, and relative magnitude of paleosecular variation in the Phanerozoic. *Earth-Sci. Rev.*, 12:35–64.
- Kent, D. V., and Gradstein, F. M., 1985. A Cretaceous and Jurassic geochronology. *Geol. Soc. Am. Bull.*, 96:1419–1427.
- Kirschvink, J. L., 1980. The least-squares line and plane and the analysis of palaeomagnetic data. *Geophys. J. R. Astron. Soc.*, 62:699–718.
- Kono, M., 1980. Statistics of paleomagnetic inclination data. *J. Geophys. Res.*, 85:3878–3882.
- Lancelot, Y., Larson, R., et al., 1990. *Proc. ODP, Init. Repts.*, 129: College Station, TX (Ocean Drilling Program).
- Larson, R. L., Schlanger, S. O., et al., 1981. *Init. Repts. DSDP*, 61: Washington (U.S. Govt. Printing Office).
- Moberly, R., Schlanger, S. O., et al., 1986. *Init. Repts. DSDP*, 89: Washington (U.S. Govt. Printing Office).
- Nagata, T., 1961. *Rock Magnetism*: Tokyo (Maruzen Co.), 350.
- Ogg, J. G., Kodama, K., Wallick, B. P., 1991. Lower Cretaceous magnetostratigraphy off northwest Australia (DSDP Site 261 and ODP Site 765, Argo Abyssal Plain, and ODP Site 766, Gascoyne Abyssal Plain). In Gradstein, F. M., Ludden, J. N., et al., *Proc. ODP, Sci. Results*, 123: College Station, TX (Ocean Drilling Program).
- Ozima, M., Saito, K., and Takigami, Y., 1981. ^{40}Ar - ^{39}Ar Geochronological studies on rocks drilled at Holes 462 and 462A, Deep Sea Drilling Project Leg 61. In Larson, R. L., Schlanger, S. O., et al., *Init. Repts. DSDP*, 61: Washington (U.S. Govt. Printing Office), 701–704.
- Schaaf, A., 1986. Radiolaria from deep sea drilling project Leg 89. In Moberly, R., Schlanger, S. O., et al., *Init. Repts. DSDP*, 89: Washington (U.S. Govt. Printing Office), 321–326.
- Shipboard Scientific Party, 1986. Site 462. In Moberly, R., Schlanger, S. O., et al., 1986. *Init. Repts. DSDP*, 89: Washington (U.S. Govt. Printing Office), 157–212.
- , 1990. Site 802. In Lancelot, Y., Larson, R. L., et al., *Proc. ODP, Init. Repts.*, 129: College Station, TX (Ocean Drilling Program), 171–243.
- Shive, P. N., 1986. Suggestions for the use of SI units in magnetism. *Eos*, 67:25.
- Stacey, F. D., and Banerjee, S. K., 1974. *The Physical Principles of Rock Magnetism*: Amsterdam (Elsevier).
- Steiner, M. B., 1981. Paleomagnetism of the igneous complex, Site 462. In Larson, R. L., Schlanger, S. O., et al., 1981. *Init. Repts. DSDP*, 61: Washington (U.S. Govt. Printing Office), 717–730.

Date of initial receipt: 13 June 1991

Date of acceptance: 30 January 1992

Ms 129B-134

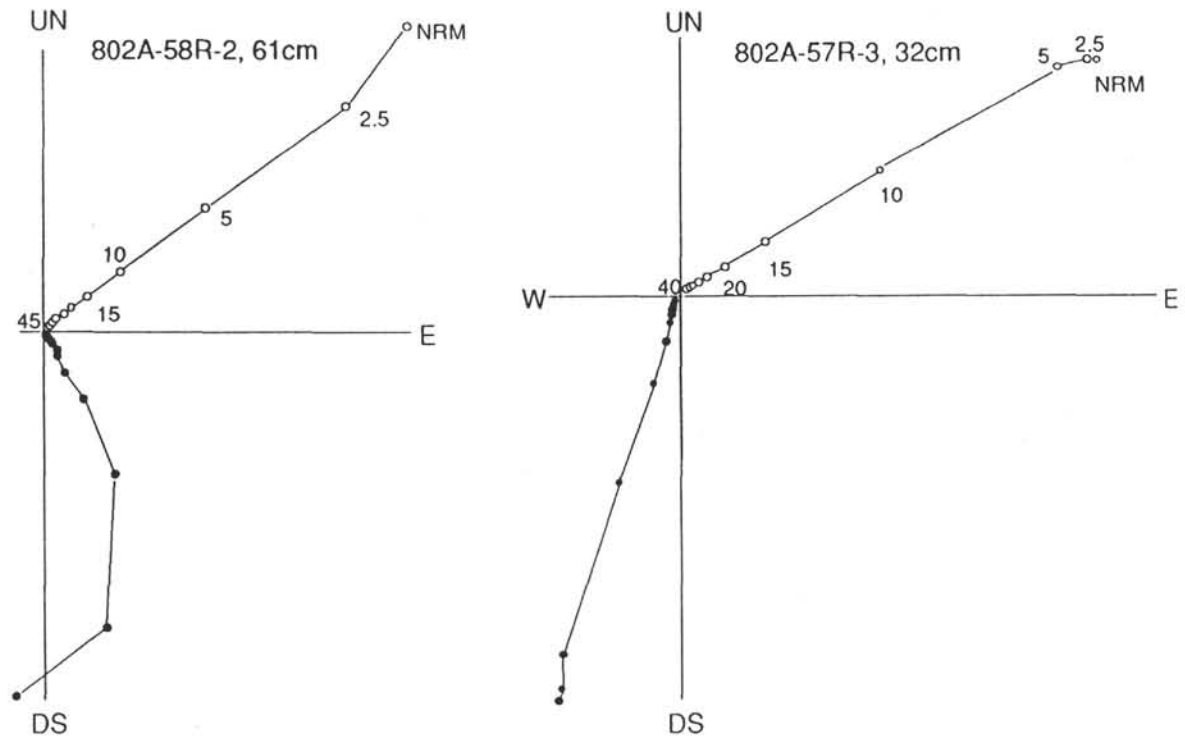


Figure 4. Zijderveld vector plots of samples illustrating the uniform decay of vectors typical of most samples analyzed in this set.

APPENDIX

Sample (cm)	AF step (Oe)	Declination (degrees)	Inclination (degrees)	Intensity (A/m)
802A-57R-2, 119	0	98.2	-1.8	16.4545
	25	97.2	-20.1	20.0909
	50	97.5	-20.7	18.1818
	100	97.1	-21.3	7.9909
	150	96.9	-21.7	2.8091
	200	96.6	-21.9	1.2909
	250	115.6	-27.9	0.5527
	300	96.6	-22.6	0.3909
	350	96.1	-25.2	0.2436
	400	96.0	-46.7	0.0973
	450	98.2	-26.7	0.1036
500	94.2	-34.1	0.0768	
802A-57R-3, 32	0	197.3	-28.9	28.4545
	25	196.9	-29.6	28.0909
	50	197.5	-30.7	26.1818
	100	197.0	-31.7	13.9091
	150	196.9	-32.0	6.0000
	200	195.7	-31.6	3.2000
	250	195.8	-31.5	1.9364
	300	195.3	-31.6	1.3273
	350	194.8	-31.8	0.9727
	400	194.2	-31.4	0.7255
	450	194.2	-31.6	0.5600
500	193.3	-32.2	0.4445	
802A-58R-1, 6	0	280.1	-35.0	19.8182
	25	279.8	-35.3	19.1818
	50	281.3	-36.3	13.9091
	100	281.6	-36.1	5.3636
	150	275.7	-35.5	2.4182
	200	282.0	-36.1	1.4545
	250	282.9	-38.0	1.0545
	300	280.9	-35.2	0.6582
	350	282.7	-35.5	0.4773
	400	282.3	-14.1	0.2782
	450	275.5	-32.4	0.2400
802A-58R-2, 15	0	228.2	-27.9	3.8636
	25	225.5	-32.0	3.2182
	50	226.5	-35.7	2.0818
	100	226.3	-37.2	0.9727
	150	225.6	-38.5	0.5064
	200	225.9	-36.3	0.2727
	250	229.7	-40.0	0.1400
	300	220.6	-41.7	0.1000
	350	221.6	-39.8	0.0623
	400	210.0	-51.8	0.0377
	450	238.6	-40.3	0.0359
802A-58R-2, 61	0	184.2	-37.6	6.4727
	25	167.5	-36.7	5.2636
	50	153.7	-37.7	2.8545
	100	150.5	-39.1	1.4091
	150	150.9	-39.2	0.8191
	200	148.3	-39.6	0.5227
	250	147.2	-38.0	0.3927
	300	147.9	-39.5	0.2373
	350	146.2	-38.1	0.1809
	400	149.0	-42.3	0.1382
	450	150.3	-43.4	0.0839
500	155.7	-48.3	0.0630	
802A-58R-2, 134	0	247.3	-32.6	15.5455
	25	247.9	-30.9	15.5455
	50	248.2	-31.0	15.1818
	100	248.5	-30.7	10.8182
	150	247.4	-30.8	5.2364
	200	246.8	-30.3	2.6364
	250	246.2	-29.0	1.3727
	300	245.6	-27.8	0.7791
	350	245.0	-26.6	0.4827
	400	244.8	-25.4	0.3118
	450	243.6	-25.9	0.2091
500	244.4	-25.9	0.1491	
802A-58R-3, 6	0	208.2	-38.2	8.1091

Appendix (continued).

Sample (cm)	AF step (Oe)	Declination (degrees)	Inclination (degrees)	Intensity (A/m)
802A-58R-3, 58	25	208.4	-37.6	8.0364
	50	208.3	-38.0	7.9273
	100	209.1	-36.5	5.5636
	150	210.2	-35.6	2.5182
	200	210.5	-32.6	1.2273
	250	211.7	-29.1	0.6100
	300	212.2	-24.6	0.3236
	350	211.8	-21.4	0.1982
	400	214.0	-19.8	0.1236
	450	224.5	-25.5	0.0689
	802A-58R-4, 51	0	180.3	-17.2
25		186.5	-19.3	9.0636
50		186.7	-19.4	7.6818
100		186.5	-19.9	3.3091
150		186.5	-20.0	1.2909
200		186.4	-19.4	0.6364
250		186.6	-19.3	0.3482
300		186.3	-19.3	0.2036
350		185.6	-20.2	0.1182
400		189.1	-25.7	0.0623
802A-58R-4, 92		0	321.9	-21.9
	25	291.9	-21.4	14.5455
	50	289.9	-21.0	11.8182
	100	289.3	-21.3	4.8818
	150	289.0	-22.1	1.8727
	200	289.5	-22.0	0.8809
	250	238.8	-6.6	0.2909
	300	286.0	-22.7	0.2700
	350	288.6	-20.9	0.1691
	400	286.9	-22.8	0.1091
	802A-59R-1, 20	0	95.4	25.8
25		35.0	-4.5	6.6091
50		46.5	-26.3	5.2909
100		50.8	-33.0	3.2364
150		52.5	-34.4	2.2909
200		51.8	-35.1	1.7818
250		52.9	-34.3	1.3455
300		52.2	-35.4	1.0727
350		51.6	-35.5	0.8764
400		51.3	-37.2	0.7136
450		55.0	-36.5	0.5509
500	53.4	-35.2	0.4509	
550	67.9	-24.9	0.2973	
600	49.8	-31.9	0.3027	
802A-59R-1, 119	0	107.3	-46.1	3.8364
	25	343.0	-34.8	11.2727
	50	342.7	-38.0	9.0909
	100	341.3	-40.6	4.8182
	150	341.9	-40.8	2.8727
	200	342.4	-40.5	2.0273
	250	342.5	-40.6	1.5727
	300	342.9	-40.4	1.2545
	350	342.6	-40.6	1.0455
	400	343.0	-40.3	0.8518
	450	343.0	-39.9	0.7255
500	344.3	-38.9	0.5927	
550	343.1	-39.5	0.4964	
600	343.5	-40.2	0.4127	
802A-59R-2, 63	0	217.4	28.8	16.0909
	25	343.6	-41.0	23.4545

Appendix (continued).

Sample (cm)	AF step (Oe)	Declination (degrees)	Inclination (degrees)	Intensity (A/m)
	50	343.4	-40.9	23.0909
	100	343.8	-41.0	17.5455
	150	344.0	-40.6	10.4545
	200	345.2	-39.6	6.1818
	250	345.9	-38.3	3.7000
	300	346.9	-36.9	2.3636
	350	347.7	-35.3	1.6273
	350	348.1	-34.4	1.1818
	450	349.1	-33.1	0.9064
	500	350.2	-31.9	0.7345
	550	350.7	-31.2	0.5891
	600	351.6	-30.8	0.4864
802A-59R-2, 135	0	46.5	-5.1	4.6636
	25	314.9	-29.6	11.2727
	50	314.1	-27.9	9.6364
	100	313.3	-38.0	5.3727
	150	315.9	-31.4	1.8909
	200	316.2	-30.9	0.9727
	250	316.9	-29.3	0.5427
	300	315.9	-29.6	0.3482
	300	317.0	-28.5	0.2336
	400	317.3	-27.2	0.1636
	450	309.7	-25.3	0.1245
	500	4.9	-77.8	0.0392
802A-59R-3, 124	0	90.8	-65.3	10.0909
	0	91.2	-46.9	12.1818
	25	90.8	-47.0	12.0909
	50	90.5	-47.2	11.0909
	100	90.2	-46.8	5.9545
	150	90.0	-45.4	2.9364
	200	89.8	-44.6	1.7000
	250	87.7	-43.4	1.0909
	300	89.4	-42.3	0.7718
	350	90.8	-42.0	0.5745
	400	90.0	-41.6	0.4182
802A-60R-1, 7	0	260.9	-2.8	2.3636
	0	42.4	-43.7	9.5455
	25	42.7	-44.6	9.4545
	50	43.4	-45.1	8.3182
	100	43.4	-45.4	4.2273
	150	45.2	-44.1	1.9182
	200	45.7	-42.4	1.0182
	250	46.1	-41.1	0.6145
	300	45.9	-39.8	0.4191
	350	47.1	-39.7	0.3018
	400	47.6	-39.3	0.2236
	450	46.5	-38.2	0.1727
	500	49.1	-40.6	0.1382
802A-60R-1, 26	0	119.7	22.6	6.4727
	0	3.0	-42.3	14.8182
	25	3.1	-43.2	14.4545
	50	3.0	-42.2	14.3636
	100	3.7	-44.0	9.3636
	150	4.5	-42.4	5.0455
	200	5.3	-39.4	2.9455
	250	6.0	-36.7	1.8455
	300	6.5	-34.4	1.2818
	350	6.5	-32.0	0.9273
	400	6.8	-30.7	0.7164
	450	6.9	-29.5	0.5709
	500	7.9	-28.5	0.4427
	550	7.8	-27.8	0.3600
	600	8.3	-27.7	0.2973
	650	7.2	-26.9	0.2445
802A-61R-1, 70	0	160.0	-2.3	9.9091
	0	284.3	-34.4	28.8182
	25	284.1	-34.3	28.3636
	50	284.7	-34.5	25.0909
	100	284.4	-34.7	10.5455
	150	285.1	-35.2	4.0182
	200	285.5	-35.8	1.8909
	250	286.7	-36.2	1.0455

Appendix (continued).

Sample (cm)	AF step (Oe)	Declination (degrees)	Inclination (degrees)	Intensity (A/m)
	300	288.1	-36.7	0.6564
	350	289.4	-36.6	0.4482
	400	289.8	-37.3	0.3245
	450	292.5	-37.1	0.2445
802A-61R-1, 95	0	321.5	-16.6	1.5727
	0	126.6	-32.3	26.8182
	25	126.8	-32.9	26.7273
	50	127.1	-33.7	23.1818
	100	128.9	24.5	10.7273
	150	127.6	-33.5	6.9273
	200	128.3	-33.2	4.6636
	250	128.9	-33.3	3.4545
	300	129.4	-32.5	2.6727
	350	130.1	-32.3	2.1273
	400	130.7	-32.1	1.7182
	450	130.5	-31.9	1.4000
	500	131.0	-32.4	1.1545
	550	131.9	-32.2	0.9727
	600	131.7	-31.5	0.7955
	650	131.7	-29.7	0.6791
802A-61R-1, 145	0	224.7	32.4	8.3909
	0	115.8	-30.9	17.7273
	25	115.9	-31.4	17.0909
	50	116.2	-31.7	14.4545
	100	116.6	-31.5	6.4091
	150	117.0	-31.5	2.5909
	200	117.8	-30.5	1.2455
	250	117.4	-30.9	0.6873
	300	118.4	-30.5	0.4345
	350	116.4	-31.2	0.3009
	400	117.7	-32.1	0.2191
	450	117.4	-31.1	0.1709
802A-62R-1, 92	0	156.2	-33.5	8.3455
	25	154.7	-34.2	6.5636
	50	154.4	-36.3	4.3091
	100	153.2	-39.1	1.7364
	150	154.4	-38.1	0.7682
	200	153.5	-37.6	0.4136
	250	155.1	-35.2	0.2282
	300	154.0	-33.7	0.1564
	350	160.1	-36.9	0.0945
	400	158.3	-46.0	0.0692
	450	165.6	-21.6	0.0714
	500	152.5	-35.4	0.0379
802A-62R-1, 121	0	289.2	-20.0	4.6364
	25	220.0	-25.4	5.7455
	50	220.8	-30.1	4.2545
	100	222.3	-32.6	2.1182
	150	222.9	-32.7	1.0091
	200	223.0	-34.4	0.5445
	250	222.1	-32.4	0.3109
	300	225.2	-33.9	0.1973
	350	218.3	-35.6	0.1273
	400	219.0	-45.5	0.0982
	450	203.7	-31.3	0.0700
	500	244.5	-27.5	0.0555
	550	242.2	-53.4	0.0391
802A-62R-2, 27	0	228.1	34.6	1.9182
	0	28.6	-22.5	5.4182
	25	29.9	-32.7	4.5000
	50	31.7	-38.5	2.9727
	100	32.9	-41.9	1.3273
	150	32.1	-42.8	0.6045
	200	34.8	-45.1	0.3336
	250	34.8	-44.0	0.2000
	300	31.4	-44.3	0.1373
	350	36.1	-48.1	0.0792
	400	25.7	-47.2	0.0632
	450	24.3	-40.1	0.0516
802A-62R-2, 64	0	187.4	4.4	3.9727
	0	321.4	-28.4	10.2727

Appendix (continued).

Sample (cm)	AF step (Oe)	Declination (degrees)	Inclination (degrees)	Intensity (A/m)
	25	322.4	-33.7	9.8182
	50	322.1	-36.7	8.2909
	100	322.0	-38.3	4.9455
	150	321.7	-38.6	2.4818
	200	323.0	-38.8	1.2818
	250	321.5	-38.6	0.6718
	300	322.9	-40.7	0.3909
	350	326.2	-38.5	0.2345
	400	324.7	-40.1	0.1500
	450	325.0	-43.1	0.1191
	500	327.3	-45.0	0.0812
802A-62R-3, 23	0	165.6	88.2	3.6455
	0	218.6	-34.3	11.2727
	25	218.3	-39.0	8.7545
	50	218.2	-41.7	5.1636
	100	218.3	-44.3	2.2000
	150	217.6	-44.4	1.2000
	200	217.5	-44.5	0.5982
	250	216.5	-43.5	0.4573
	300	213.0	-43.6	0.3164
	350	217.2	-44.6	0.2227
	400	218.8	-42.0	0.1655
	450	205.6	-40.9	0.1373
	500	208.8	-49.0	0.1109